PHYSICAL REVIEW D **88,** 094001 (2013)

Three-jet production and gluon saturation effects in p-p and p-Pb collisions within high-energy factorization

A. van Hameren,* P. Kotko,† and K. Kutak‡

The H. Niewodniczański Institute of Nuclear Physics, Polish Academy of Sciences, Radzikowskiego 152, 31-342 Cracow, Poland

(Received 16 September 2013; published 4 November 2013)

We analyze three-jet production in the central-forward and forward rapidity regions in proton-proton and proton-lead collisions at LHC energies. Our calculation relies on high-energy factorization with a single off-shell gluon obeying small x evolution equation which includes saturation. The calculations are made using two independent Monte Carlo codes implementing tree-level gauge invariant off-shell matrix elements. We calculate differential cross sections for azimuthal decorrelations and unbalanced jet transverse momenta and discuss them in the context of differences in the evolution of the unintegrated gluon densities.

DOI: 10.1103/PhysRevD.88.094001 PACS numbers: 13.87.−a, 12.38.−t, 24.85.+p

I. INTRODUCTION

Jet production processes are an excellent testing ground for perturbative QCD, notably because their analysis does not require a knowledge of fragmentation functions which are subject to large errors. The only nonperturbative input that enters theoretical calculations are thus parton distribution functions (PDFs). They are defined by a particular factorization scheme; for instance, for the collinear factorization (see [1] for a review) the PDFs undergo linear Dokshitzer-Gribov-Lipatov-Altarelli-Parisi evolution equations. It is however known that at high energies reachable nowadays at LHC, certain types of logarithms occurring in the perturbative calculations can spoil the procedure. The general method is to resume those logarithms giving rise to new types of evolution equations, for instance the linear Balitski-Fadin-Kuraev-Lipatov (BFKL) equation [2,3], Catani-Ciafaloni-Fiorani-Marchesini (CCFM) [4–6], the nonlinear Balitsky and Kovchegov equation [7,8], or the nonlinear extension of the CCFM–the Kutak-Golec-Biernat-Jadach-Skrzypek equation [9,10].

An example of a situation that requires the resummation of high-energy logarithms is the production of forward jets [11–14]. Large energies and rapidities of forward jets allows us to probe the small x regime and thus it is an excellent testing ground for various resummation schemes and gluon saturation phenomenon which should occur at high-energy densities [15,16]. Forward jets are even more attractive nowadays as it is possible to study them experimentally at LHC. Thanks to dedicated forward calorimeters, the ATLAS and CMS detectors allow us to reconstruct large-transverse-momentum jets up to about five units of rapidity. This gives an opportunity to study small x effects experimentally and possibly access the kinematic region where gluon saturation may enter the game. There are indeed hints that saturation actually happens [17–20]. Various studies of forward jets were done in Refs. [21–25]. For the recent experimental studies see [26–28].

In the present paper we study three-jet production at the LHC within the high-energy factorization framework, which shall be reviewed in Sec. II. Multijet processes are interesting particularly due to a bigger phase space—by applying various cuts different properties of gluon densities can be studied. For instance by restricting two of the jets to balance each other on the transverse plane, the third jet can access the gluon transverse space directly. The detailed kinematics of the processes we consider is described in Sec. III. We present numerical results and discuss their possible interpretation in Sec. IV. Finally, we give overall summary in Sec. V.

II. FACTORIZATION AT HIGH ENERGIES

Let us now briefly recall some of the existing formalisms that may be attempted to describe the observables at high energies. Before doing so, let us, however, make some important remarks. First of all, the full control over the calculation, in particular over its limitations, can be achieved only when working within well-established factorization theorems of QCD. Besides the well-known collinear factorization there are so-called transverse-momentum-dependent (TMD) factorization theorems. They do work in certain processes (see [1]) but fail in some others. In general, they are expected to fail in hadron-hadron collisions ([29,30], see also the short summary in [31]). The TMD factorizations involve transverse-momentum-dependent gluon distribution functions, similar to those that are often used in high-energy phenomenology. The problem is, however, that the former are not universal (this is the reason the factorization is violated) whereas the latter are often conjectured to be universal. Let us thus comment on the factorization at the kinematic limit we consider in the paper, namely, the "small x" regime. It deals with dense hadronic matter (especially for collisions with heavy ions) for which

*andre.hameren@ifj.edu.pl
†piotr.kotko@ifj.edu.pl
‡krzysztof.kutak@ifj.edu.pl

the formalism of the color glass condensate (CGC) [32] proves to be very successful [18]. Basically the TMD factorizations do not deal with the small x limit, although it was shown in [33] that the universality of TMD PDFs is also violated in that limit. On the other hand, in Ref. [34] it is argued that an "effective" factorization within CGC (for dilute-dense collisions) can be seen as an instance of TMD factorization in the case of dijets production in the limit of small unbalanced transverse momentum. The factorization formula is then stated as a convolution of a few universal transverse-momentum-dependent gluon densities and matrix elements which are on shell, but use off-shell kinematics. In the large N_c limit those different gluon PDFs can be expressed in terms of two fundamental quantities: the Weizsäcker-Williams gluon density [35,36] and the "dipole" gluon density (see, e.g., [37,38] and references therein; for the possible theoretical issues of those gluon densities as seen from the TMD factorization point of view see [39,40]). Both densities are related to certain two-point Green functions. In the more general case of multiparticle production, higher correlators are needed (within CGC they are expressed by means of certain averages of the Wilson lines). However, as shown in Ref. [41] in case of dilute-dense collisions and the large N_c limit only two-point and four-point Green functions are needed. For recent applications to multiparticle production see also [42].

We see that the theoretical picture of the processes at very large densities (very small x) is complicated. Unless one is outside the saturation regime (i.e., in the BFKL or CCFM domain), only simple cases like inclusive gluon production can be described in terms of single transverse-momentum-dependent gluon density [43,44].

In the present paper we mainly concentrate on the proton-proton collisions within the kinematic region accessible by contemporary experiments. The nonlinear effects—although present—are actually rather weak. Therefore, we shall use simple k_T factorization with a single type of unintegrated gluon density, incorporating, however, the nonlinear evolution (when necessary we shall compare the results to the BFKL evolution with subleading corrections included [45]). Although simplified, such an approach was proved to be very interesting phenomenologically [20].

As a reference for the k_T factorization we take the works of Catani, Ciafaloni, and Hautmann (CCH) [46–51] (the following type of factorization formula appeared also much earlier in [15]). Originally it was stated for heavy quark pair production at tree level; however, we shall assume that one can extend it for more complicated final states including gluons, with the complications explained below. The factorization is expressed by the following formula [see Fig. 1(a)]; for some partonic final state X and two initial state hadrons A, B we have

$$d\sigma_{AB\to X} = \int \frac{d^2k_{TA}}{\pi} \int \frac{dx_A}{x_A} \int \frac{d^2k_{TB}}{\pi} \int \frac{dx_B}{x_B} \mathcal{F}_{g^*/A}(x_A, k_{TA}) \times \mathcal{F}_{g^*/B}(x_B, k_{TB}) d\hat{\sigma}_{g^*g^*\to X}(x_A, x_B, k_{TA}, k_{TB}), \tag{1}$$

where $\mathcal{F}_{g^*/H}$ are transverse-momentum-dependent densities of the off-shell gluons g^* inside H (to be discussed below) and $\hat{\sigma}_{g^*g^*\to X}$ is the high-energy hard cross section for the process $g^*(k_A)g^*(k_B) \to X$. The momenta of the off-shell gluons that enter the hard cross section are defined to be

$$k_A^\mu = x_A p_A^\mu + k_{TA}^\mu, \qquad k_B^\mu = x_B p_B^\mu + k_{TB}^\mu, \tag{2}$$

where $p_A \cdot k_T = p_B \cdot k_T = 0$. The hard amplitude with the external off-shell gluons is defined by means of certain high-energy (or eikonal) projectors, i.e., the off-shell leg (including the propagator) with momentum k_A, k_B is contracted with $|\vec{k}_{TA}|p_A^\mu$, $|\vec{k}_{TB}|p_B^\mu$ respectively [see Fig. 1(b)]. As already mentioned, in the original CCH works the production of a heavy quark pair was considered. In that case the corresponding off-shell amplitude is gauge invariant, fundamentally due to the form of the projectors. This is, however, not true for the off-shell amplitudes with gluons in the final state. There are several ways to deal with this problem. First, Lipatov's effective action [52] and the resulting Feynman rules [53] can be used. This is because the kinematics (2) corresponds to quasi-multi-Regge kinematics in the terminology of [53] (for recent

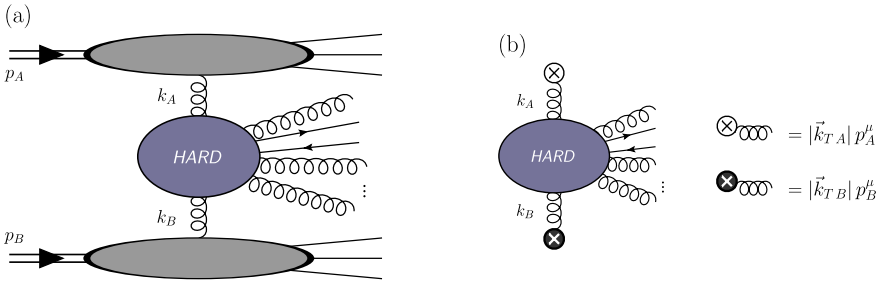

FIG. 1 (color online). (a) Factorization of a hadronic collision into unintegrated PDFs (top and bottom blobs after "squaring") and a parton-level subprocess (middle blob). (b) The hard subprocess is defined by off-shell matrix elements with incoming off-shell gluon propagators contracted with high-energy projectors (explained on the rhs). In order to make this amplitude gauge invariant, additional contributions are needed (see the main text).

LHC-related calculations in that framework we refer, e.g., to [54–56]). A second approach developed recently in [57] is suitable for automatic calculation of large final state multiplicities and uses a manifestly gauge invariant method of embedding the off-shell process in a larger on-shell process without compromising high-energy kinematics. Finally, there is one more approach [58] suitable in a simplified situation described later in this section.

In the CCH approach, the transverse-momentum-dependent gluon densities $\mathcal{F}_{g^*/H}$ were originally assumed to undergo the BFKL evolution. As we have remarked above, we shall use the formula (1) with $\mathcal{F}_{g^*/H}$ incorporating more subtle effects, in particular gluon saturation. In the present paper we shall use the nonlinear Balitsky and Kovchegov equation, extended with a consistency constraint, a nonsingular piece of the gluon splitting function and running a strong coupling constant [59,60]. The strength of the nonlinearity is adjusted by a parameter that can be interpreted as a radius of a hadron, either proton or nuclei (e.g., in Ref. [20] it was applied for a lead target). Let us remark that since there is a conjecture that the integration of $\mathcal{F}_{g^*/H}$ over the transverse momentum is related to a collinear PDF, we shall often refer to $\mathcal{F}_{g^*/H}$ as the unintegrated gluon density. The relation between both quantities reads

$$\int dk_{TA}^2 \mathcal{F}_{g^*/A}(x_A, k_{TA}) = x_A f_{g/A}(x_A). \tag{3}$$

Suppose now that we deal with asymmetric kinematics, i.e., $x_B \gg x_A$, which is a characteristic feature of forward scattering (see the next section). Then the gluon originating from hadron B is probed near the mass shell and $\mathcal{F}_{g^*/B}$ should be replaced by its collinear equivalent $f_{g/B}$. Moreover, the valence quarks play an important role. Thus, the proper formula in such a setup is given by

$$d\sigma_{AB\to X} = \int \frac{d^2k_{TA}}{\pi} \int \frac{dx_A}{x_A} \int dx_B \sum_b \mathcal{F}_{g^*/A}(x_A, k_{TA}) f_{b/B}(x_B) \times d\hat{\sigma}_{g^*b\to X}(x_A, x_B, k_{TA}), \tag{4}$$

where b runs over gluon and all the quarks that can contribute to the production of multiparticle state X (see also Ref. [21] and the Appendix of [46] for the collinear limit in the high-energy factorization). In the formula above, any scale dependence was suppressed. The off-shell gauge invariant process $g^*b \to g \ldots g$ can be calculated along the lines of Ref. [58]. The case with quarks is actually straightforward, as in the axial gauge any gauge contribution due to Slavnov-Taylor identities vanishes.

Let us summarize our basic assumptions. We use the k_T-factorized, hybrid (i.e., collinear PDF is mixed with the unintegrated one, see also [61] for the CGC approach) form given in Eq. (4) with the inclusion of nonlinear effects in the evolution of the unintegrated gluon PDF. The hard matrix elements are calculated fully off shell at tree level; they are gauge invariant, and all of them are convoluted with the same gluon density given in fundamental color representation, as given in [20].

III. PROCESS DEFINITION AND KINEMATICS

Let us now give a detailed description of the process we are interested in. We want to study exclusive three-jet events, namely,

$$A(p_A)B(p_B) \to J_1(p_1)J_2(p_2)J_3(p_3), \tag{5}$$

where $A = \{p^+, \mathrm{Pb}\}$, $B = p^+$, and $J_i(p_i)$ denotes the jet with momentum p_i. We work in the c.m. frame throughout the paper. This frame corresponds to LAB frame for p^+p^+ collision, but not for the p^+Pb collisions. In our frame we define

$$p_A^\mu = (E, 0, 0, -E), \qquad p_B^\mu = (E, 0, 0, E), \tag{6}$$

with $E = \sqrt{S}/2$ where S is the total c.m. energy squared. In the present paper we consider c.m. energies $\sqrt{S} = 5.02\,\mathrm{TeV}$ and $\sqrt{S} = 7.0$ TeV.

Let us now discuss the kinematic cuts that are relevant to the physics we would like to address. To this end let us decompose the final state momenta as follows:

$$p_i^\mu = \frac{|\vec{p}_{Ti}|}{\sqrt{S}}(e^{\eta_i} p_A^\mu + e^{-\eta_i} p_B^\mu) + p_{Ti}^\mu, \tag{7}$$

where $p_{Ti} \cdot p_A = p_{Ti} \cdot p_B = 0$ and the rapidity η_i is defined as

$$\eta_i = \frac{1}{2} \ln \frac{p_i^0 + p_i^z}{p_i^0 - p_i^z}. \tag{8}$$

Further we note that

$$p_{Ti}^\mu = (0, \vec{p}_{Ti}, 0) \tag{9}$$

and

$$\vec{p}_{Ti} = (|\vec{p}_{Ti}| \sin\phi_i, |\vec{p}_{Ti}| \cos\phi_i). \tag{10}$$

Now let us come back to the kinematic cuts. First of all we assume that

$$|\vec{p}_{Ti}| > p_{T\mathrm{cut}}, \qquad i = 1, 2, 3. \tag{11}$$

The actual values of the cuts shall be given in the following sections when we discuss numerical results. Typically, we shall order the jets with decreasing $|\vec{p}_{Ti}|$ values, i.e.,

$$|\vec{p}_{T1}| > |\vec{p}_{T2}| > |\vec{p}_{T3}|. \tag{12}$$

Further restriction is given by a jet definition. Here we work with an anti-k_T clustering algorithm [62] with radius R_{cut}; thus, the final state momenta cannot be too close in the ϕ-η space.[1] In order to access the small x region we

[1]Actually for tree-level parton-level processes it is equivalent to a proper cut on the ϕ-η plane.

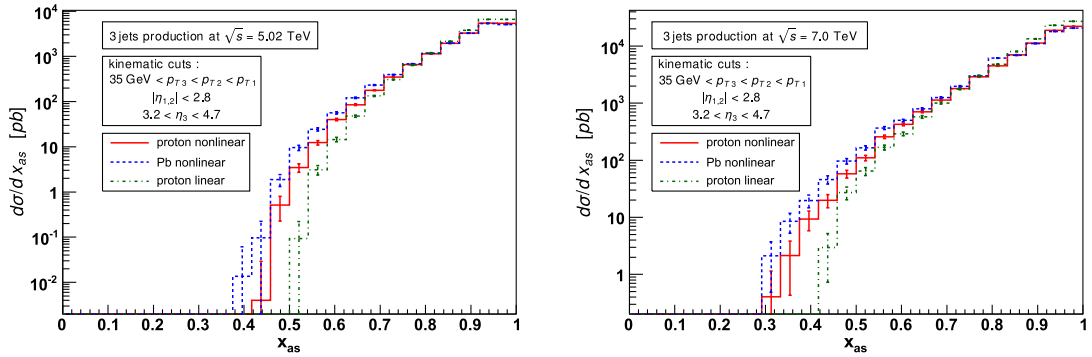

FIG. 2 (color online). The differential cross section as a function of asymmetry variable x_{as} for the forward-central rapidity region and two different c.m. energies: left for 5.02 TeV, right for 7.0 TeV.

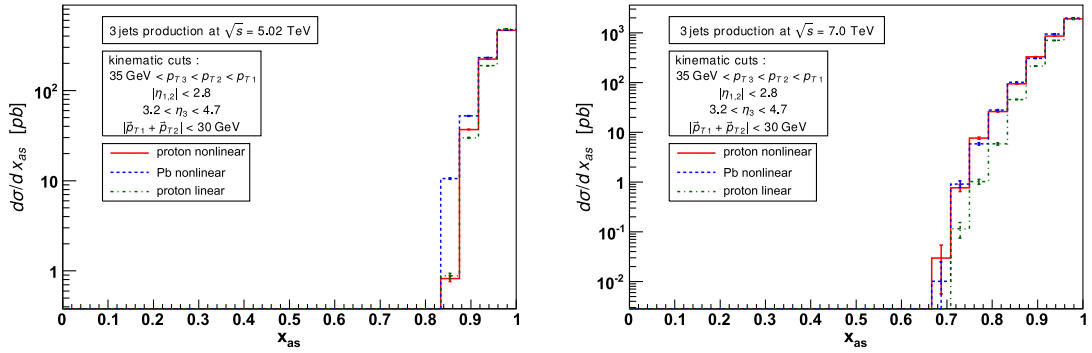

FIG. 3 (color online). The differential cross section as a function of asymmetry variable x_{as} for the forward-central rapidity region with the back-to-back cut $D_{\mathrm{cut}} = 30$ GeV and two different c.m. energies: left for 5.02 TeV, right for 7.0 TeV.

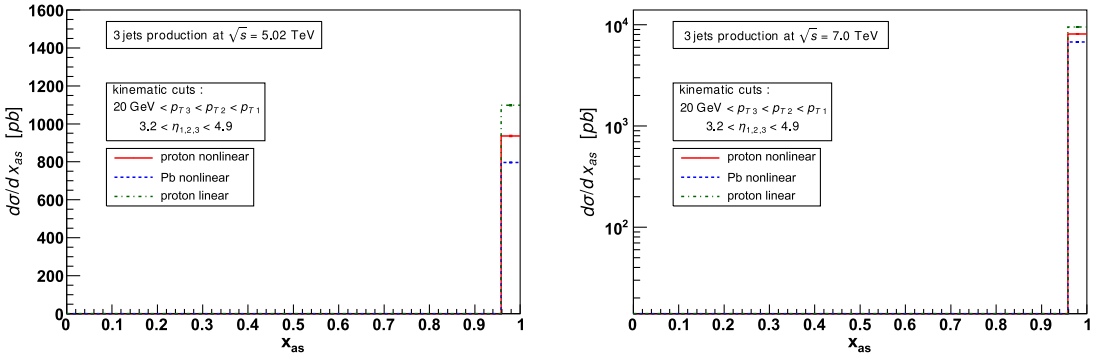

FIG. 4 (color online). The differential cross section as a function of asymmetry variable x_{as} for the purely forward rapidity region and two different c.m. energies: left for 5.02 TeV, right for 7.0 TeV.

have to impose additional cuts. According to (7) and the factorization formula [cf. Eq. (2)], the longitudinal fractions of the hadrons' momenta x_A, x_B that initiate the hard scattering are given by

$$x_A = \sum_i \frac{|\vec{p}_{Ti}|}{\sqrt{S}} e^{\eta_i}, \qquad x_B = \sum_i \frac{|\vec{p}_{Ti}|}{\sqrt{S}} e^{-\eta_i}. \tag{13}$$

Thus, in order to select small, say, x_A for the fixed S and $|\vec{p}_{Ti}|$ we have to go to large rapidity values, ideally for all the jets. In the same time x_B, would be large; thus, this sort of kinematics is often referred to as *asymmetric kinematics*. If some of the jets appear in the central rapidity region, we can still access the small x regime provided at least one of the jets is in the forward region. Those issues shall be illustrated by a specific calculation in Sec. IV B. The forward region is defined as

$$\eta_{f0} \leq \eta_i \leq \eta_{f1}, \tag{14}$$

while the central region is defined as

$$|\eta_j| \leq \eta_c, \tag{15}$$

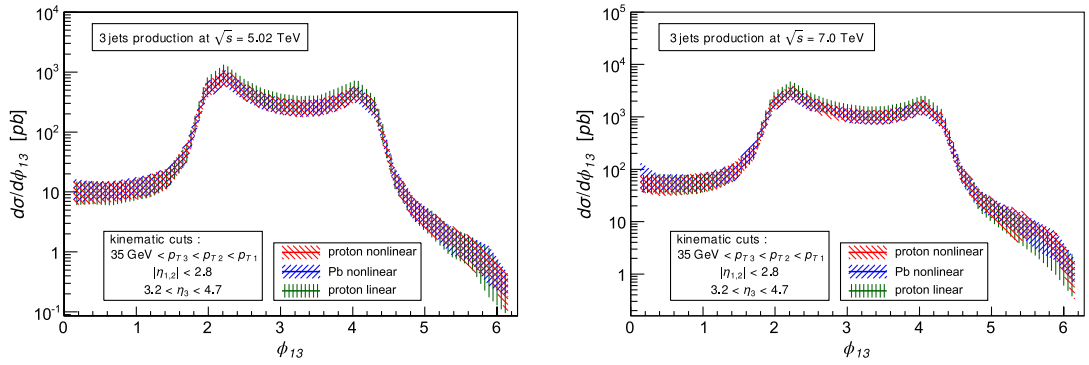

FIG. 5 (color online). Differential cross section in difference of the azimuthal angles between the leading and forward jets. The band represents the theoretical uncertainty due to scale variation and statistical errors. The left plot corresponds to c.m. energy 5.02 TeV, the right to 7.0 TeV.

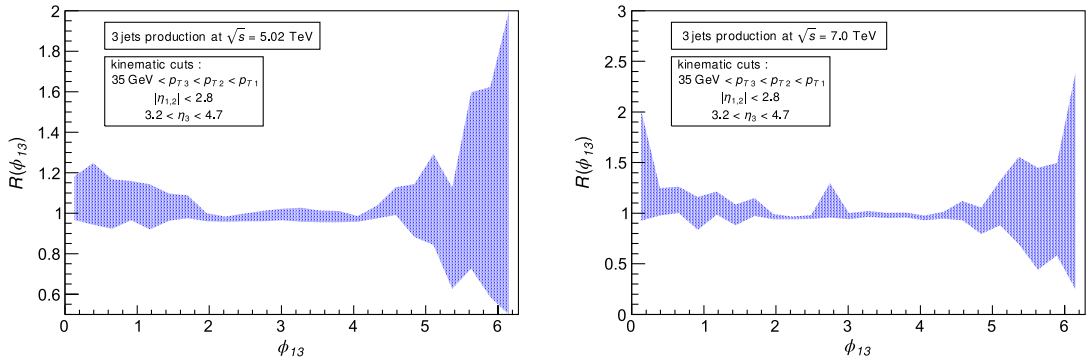

FIG. 6 (color online). The nuclear modification factor as a function of the difference of the azimuthal angles between the leading and forward jets. The band represents the theoretical uncertainty due to scale variation and statistical errors. The left plot corresponds to c.m. energy 5.02 TeV, the right to 7.0 TeV.

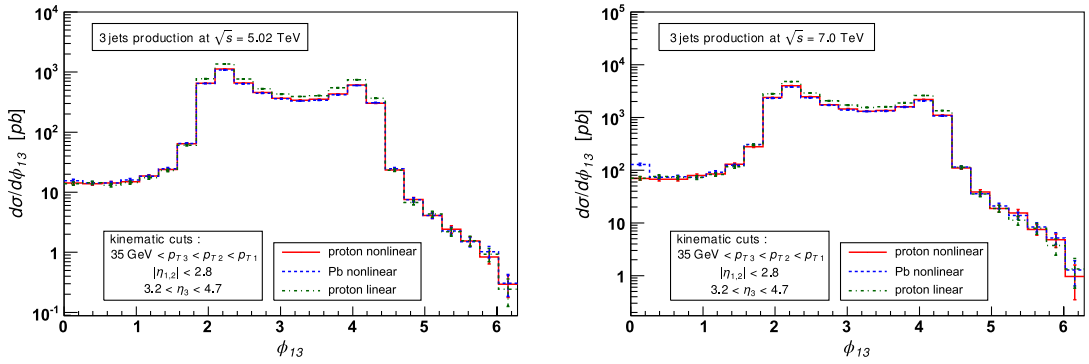

FIG. 7 (color online). Differential cross section in difference of the azimuthal angles between the leading and forward jets for a particular choice of the scale $\mu/2$. The eft column corresponds to c.m. energy 5.02 TeV, the right to 7.0 TeV.

with specific boundary values η_{f0}, η_{f1}, η_c given later. Note, that we tag the forward jet in the positive rapidity hemisphere only, both for proton-proton and proton-lead collisions.

There are also additional cuts that might be interesting for the studies of unintegrated gluon densities. We may restrict the two leading jets to be back-to-back-like. More precisely, we can define

$$p_{T12} = |\vec{p}_{T1} + \vec{p}_{T2}| < D_{\text{cut}}, \tag{16}$$

with the D_{cut} parameter being not much smaller then $p_{T\text{cut}}$. Such a study is motivated by the fact that for $D_{\text{cut}} \to 0$ the total transverse momentum of the initial state gluons is transferred to the forward jet.

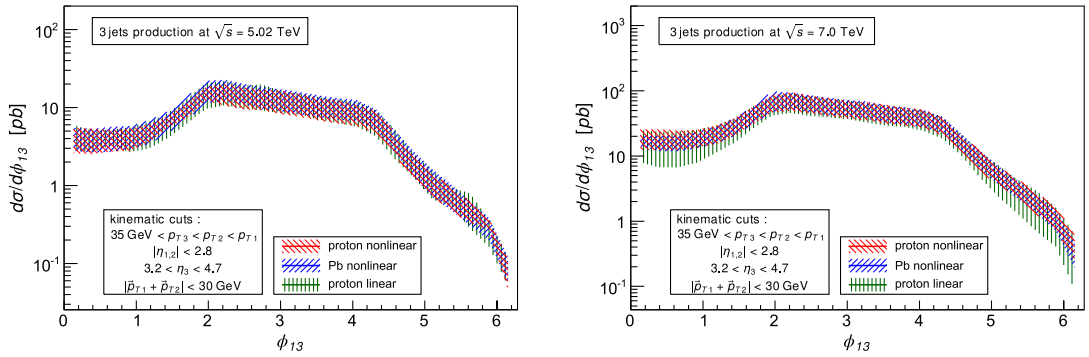

FIG. 8 (color online). Differential cross section in difference of the azimuthal angles between the leading and forward jets with the additional restriction that the two leading jets are back-to-back-like. The band represents the theoretical uncertainty due to scale variation and statistical errors. The left plot corresponds to c.m. energy 5.02 TeV, the right to 7.0 TeV.

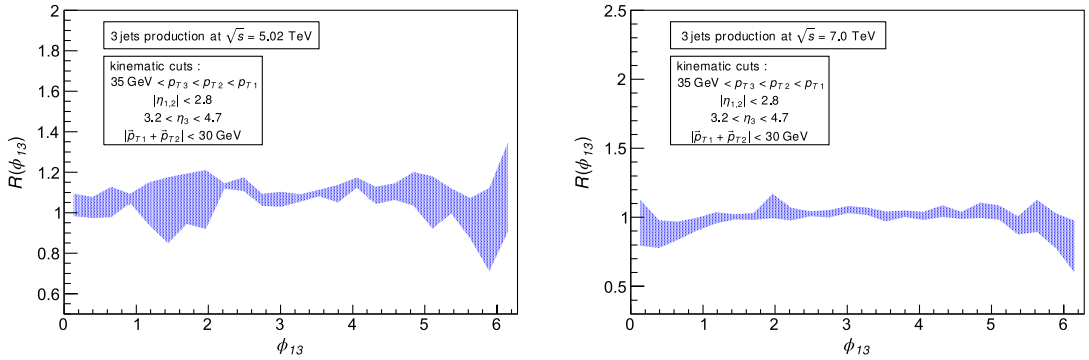

FIG. 9 (color online). The nuclear modification factor as a function of the difference of the azimuthal angles between the leading and forward jets, with the additional restriction that the two leading jets are back-to-back-like. The band represents the theoretical uncertainty due to the scale variation and statistical errors. The left plot corresponds to c.m. energy 5.02 TeV, the right to 7.0 TeV.

IV. NUMERICAL RESULTS AND DISCUSSION

A. Preliminary remarks

The numerical calculations were performed using two new Monte Carlo programs and were cross-checked against each other. The first program is a C++ code using the FOAM algorithm [63] and based on the method for the off-shell matrix elements described in Ref. [58]. The working name of the program is LxJet.[2] The second independent code is a FORTRAN program based on [57]. Since we want to study some small x properties of the jet observables within high-energy factorization itself, we do not interface the program with any parton shower in the present calculation. The final state parton shower can be added using, e.g., PYTHIA [64] and shall be done in the future. Another shortcoming comes from neglecting multiple parton interactions (MPIs). Contrary to dijet production, where MPIs lead to a change of the overall normalization of angle distributions [65], the situation for three-jet production is more complicated and is left for further study.

[2]The program shall be publicly available.

Let us now summarize the inputs we have used. For the unintegrated parton densities $\mathcal{F}_{g^*/H}$ we take the ones described in the previous section and fitted to HERA data in [20]. These include the nonlinear PDFs for proton, lead, and additionally the proton PDF with linear evolution [45]. For the collinear PDFs f_a we take the CTEQ10 next-to-leading order set [66]. The consistent strong coupling constant is also taken from the same source. Since our calculations are essentially tree level as far as the parton-level amplitude is concerned, there is a large dependence on the choice of the scales. In order to estimate the theoretical uncertainty we do the following standard procedure. First, we set the renormalization and collinear factorization scales to be equal $\mu_f = \mu_r \equiv \mu$ and choose

$$\mu = E_1 + E_2 + E_3. \tag{17}$$

Our error estimate is then given by the band constructed from the two outputs with the two choices of the scale (including statistical errors): $\mu/2$ and 2μ. In all calculations we choose the radius of the anti-k_T algorithm to be $R_{\text{cut}} = 0.5$.

We consider two rapidity configurations:

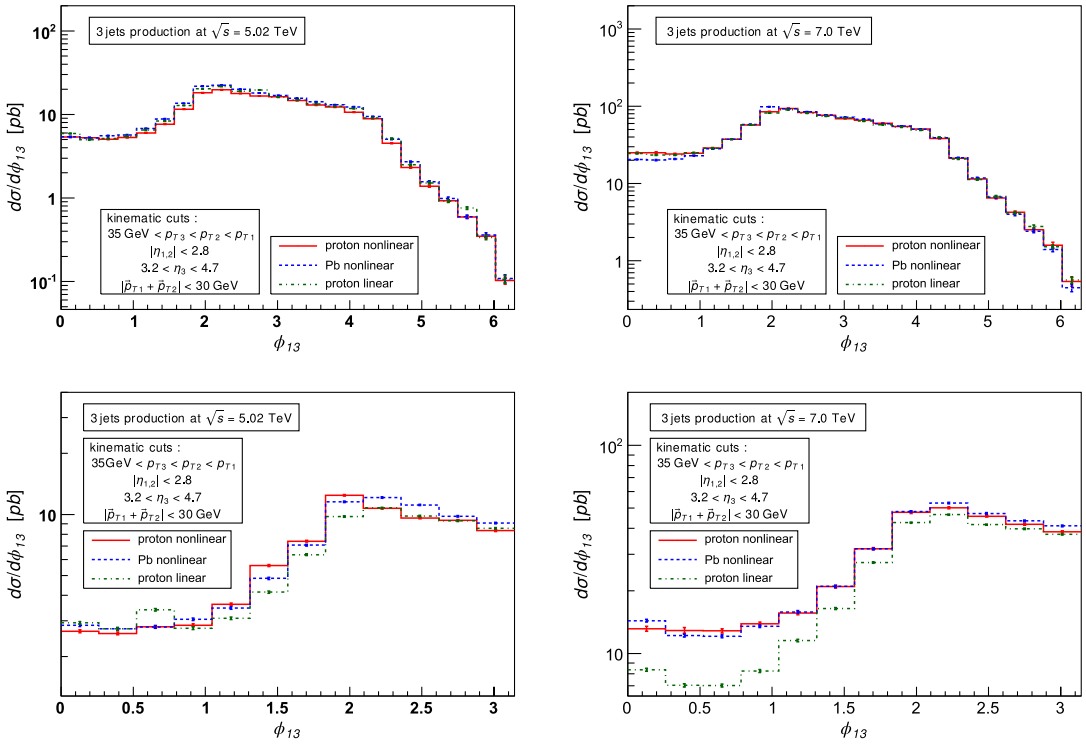

FIG. 10 (color online). Differential cross section in difference of the azimuthal angles between the leading and forward jets, with the additional restriction that the two leading jets are back-to-back-like. The left column corresponds to c.m. energy 5.02 TeV, the right to 7.0 TeV. The top plots are made for the scale $\mu/2$ and $0 < \phi_{13} < 2\pi$ while the bottom for the scale 2μ and $0 < \phi_{13} < \pi$.

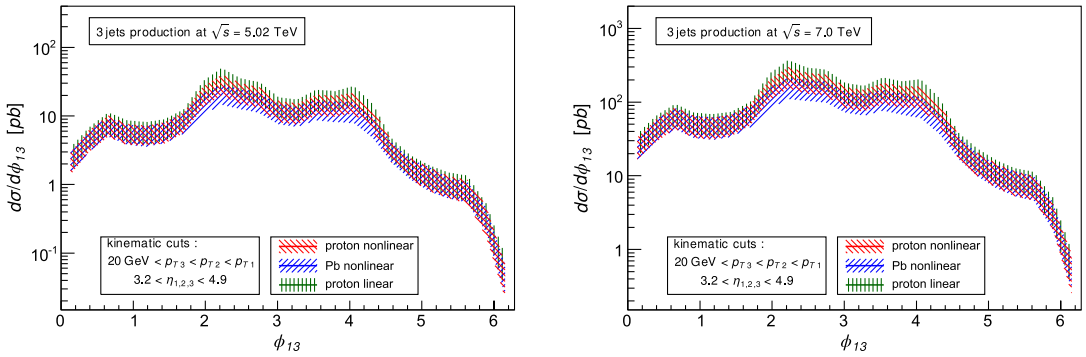

FIG. 11 (color online). Differential cross section in difference of the azimuthal angles between the leading and forward jets for the forward rapidity region. The band represents the theoretical uncertainty due to scale variation and statistical errors. The left plot corresponds to c.m. energy 5.02 TeV, the right to 7.0 TeV.

(i) *central-forward region*: we demand that the two hardest jets (with indices 1, 2) are in the central region defined by $\eta_c = 2.8$, while the softest jet (with index 3) is in the forward region defined by $\eta_{f0} = 3.2$, $\eta_{f1} = 4.7$,

(ii) *forward region*; all three jets are within the region defined by $\eta_{f0} = 3.2$, $\eta_{f1} = 4.9$.

B. Asymmetry distributions

In order to check if the region of the longitudinal fractions x_A, x_B we access is consistent with our assumptions leading to Eq. (4) let us we define the following variable:

$$x_{\rm as} = \frac{|x_A - x_B|}{x_A + x_B}. \tag{18}$$

It has the support in [0, 1] and measures the asymmetry of the event (for $x_{\rm as} \to 1$ we have totally asymmetric events). We expect that within our kinematic cuts the cross section is dominated by asymmetric events, being thus in agreement with Eq. (4). This point shall be verified by explicit calculations below.

In Figs. 2–4 we present differential cross sections in $x_{\rm as}$ for three different scenarios: the forward-central rapidity region, the forward-central region with two leading jets

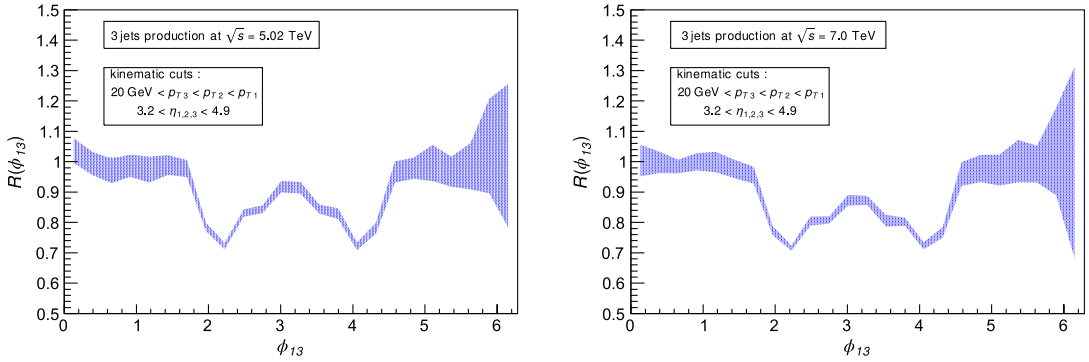

FIG. 12 (color online). The nuclear modification factor as a function of the difference of the azimuthal angles between the leading and forward jets for the forward rapidity region. The band represents the theoretical uncertainty due to scale variation and statistical errors. The left plot corresponds to c.m. energy 5.02 TeV, the right to 7.0 TeV.

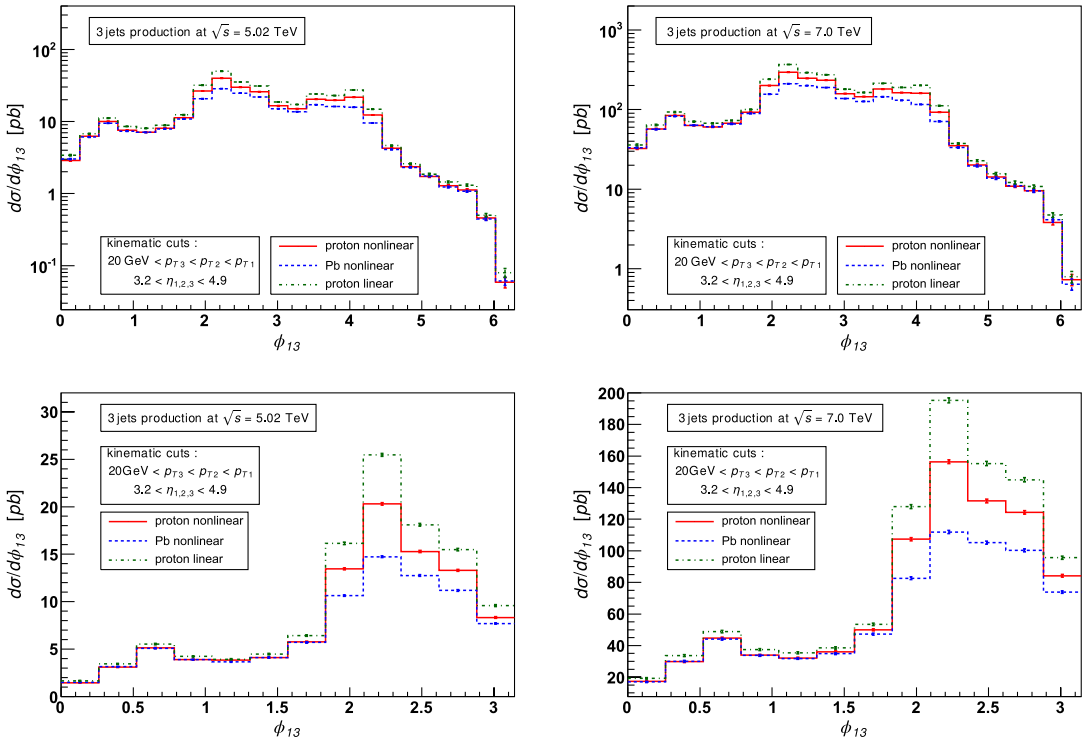

FIG. 13 (color online). Differential cross section in difference of the azimuthal angles between the leading and forward jets for the forward rapidity region. The left column corresponds to c.m. energy 5.02 TeV, the right to 7.0 TeV. The top plots are made for the scale $\mu/2$ and $0 < \phi_{13} < 2\pi$ while the bottom for the scale 2μ and $0 < \phi_{13} < \pi$.

being close to back to back, and the purely forward region. The rapidity regions were defined in the previous section. Further details are given in the plots. We see that the collisions in the forward region (Fig. 4) are completely asymmetric as one should expect. However, most of the events in the forward-central region are also asymmetric, as seen in Fig. 2. We have observed, that—as far as the forward-central collisions are concerned—lowering the $p_{T\text{cut}}$ spoils the asymmetry of the events; thus, one cannot go to as low $p_{T\text{cut}}$ as for purely forward collisions.

C. Azimuthal decorrelations

1. Central-forward jets

Let us now present the results for azimuthal decorrelations for central-forward jet configuration. There are many azimuthal observables that can be studied within this context. In this paper we study distributions in the azimuthal angle between the leading jet (with index 1) and the softest jet (with index 3)

$$\phi_{13} = |\phi_1 - \phi_3|, \qquad \phi_{13} \in [0, 2\pi). \tag{19}$$

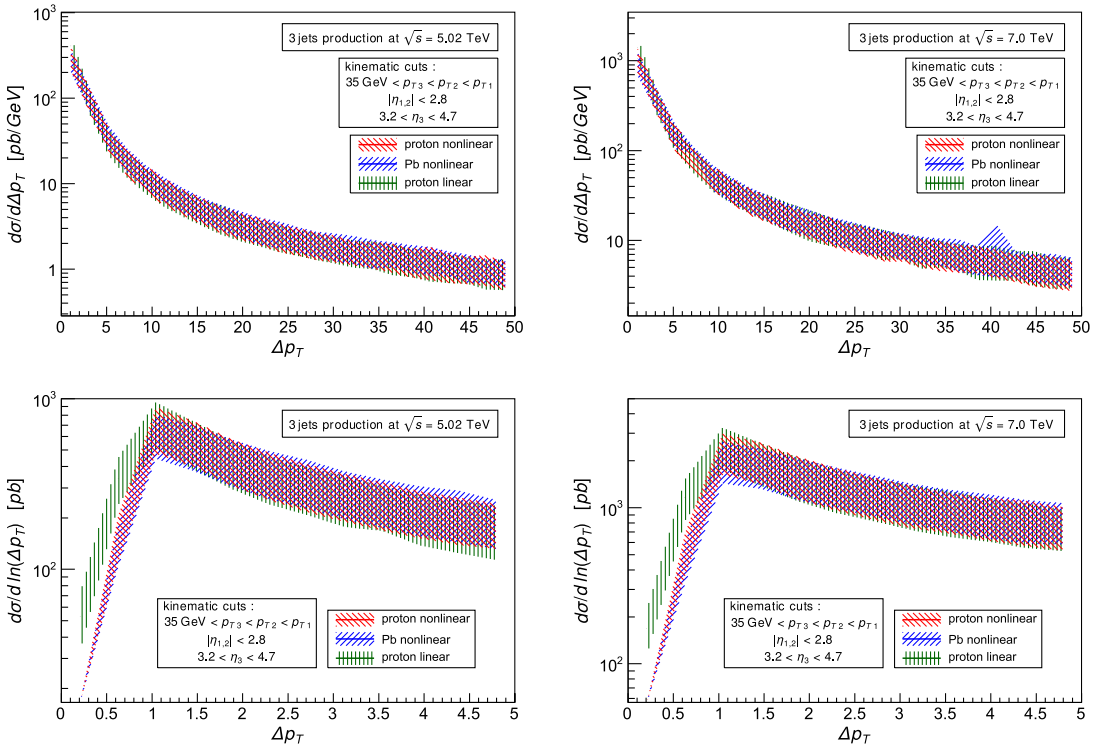

FIG. 14 (color online). Differential cross section in the unbalanced p_T for central-forward jets. The band represents the theoretical uncertainty due to scale variation and statistical errors. The left plots correspond to c.m. energy 5.02 TeV, the right to 7.0 TeV. The bottom plots zoom the low Δp_T region [note the distributions are differential in $\ln(\Delta p_T)$ there].

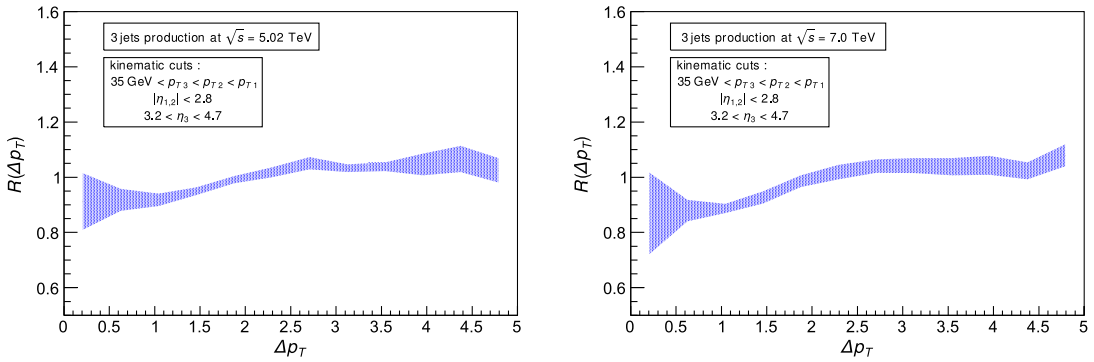

FIG. 15 (color online). The nuclear modification factor for central-forward jets as a function of the unbalanced p_T for the region close to zero. The band represents the theoretical uncertainty due to scale variation and statistical errors. The left plot corresponds to c.m. energy 5.02 TeV, the right to 7.0 TeV.

Note that this angle is always calculated in one direction and is not just the smallest angle between the jets. This is important; if we assume that the direction of the leading jet divides the azimuthal plane into two half-planes, the events with the forward jet lying on the left half-plane and the right half-plane (with the same smallest angle to the leading jet) are not symmetric. Let us note that in the collinear factorization at leading order the momentum conservation requires that $\pi/2 < \phi_{13} < 3\pi/2$. Thus, the shapes given in the plots discussed below are a characteristic feature of the high-energy factorization.

In Figs. 5–7 we present a sample of our result for the differential cross section in the variable ϕ_{13}. We observe that indeed the whole region $(0, 2\pi]$ is covered by events; however, the "collinear" region $\pi/2 < \phi_{13} < 3\pi/2$ dominates. The results for the nonlinear evolution described in the Sec. II for proton and lead, as well as the BFKL with subleading corrections are similar and the nuclear modification ratio is consistent with unity, as seen in Fig. 6.

Let us now turn to the case when the two leading jets are restricted to be back-to-back-like. In the present

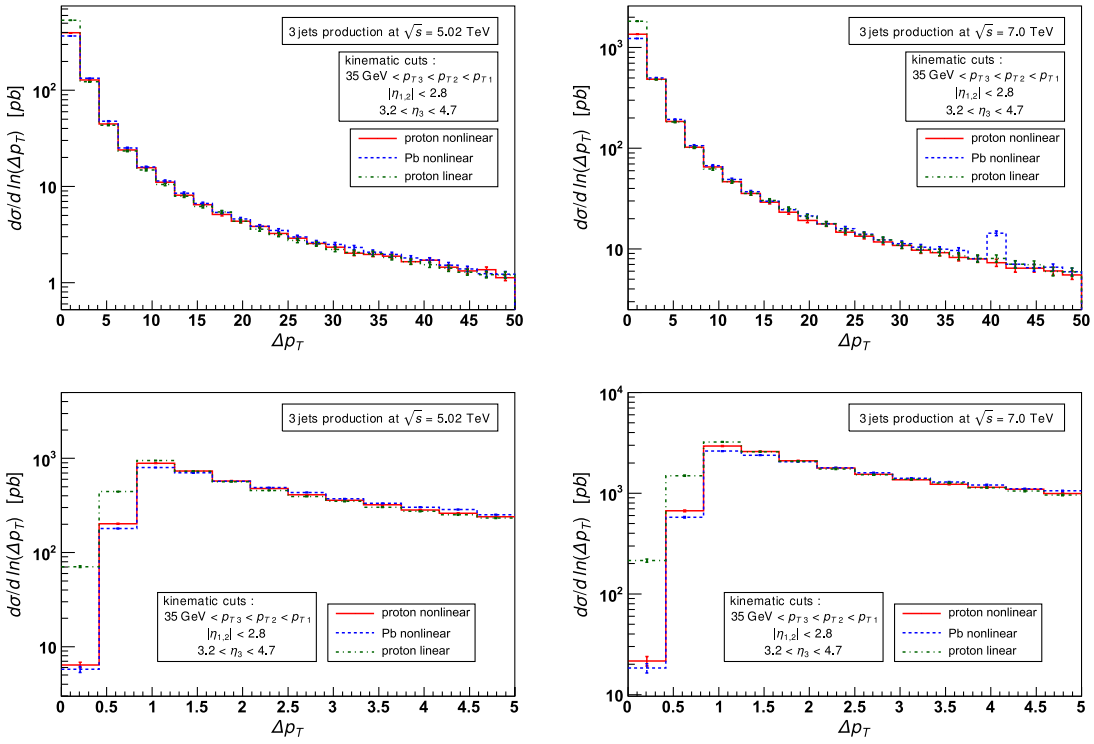

FIG. 16 (color online). Differential cross section for central-forward jets in the unbalanced p_T for a particular choice of the scale $\mu/2$. The left column corresponds to c.m. energy 5.02 TeV, the right to 7.0 TeV. The bottom plots zoom the top plots for the low Δp_T region but are calculated for the scale 2μ [note the distributions are in $\ln(\Delta p_T)$ there].

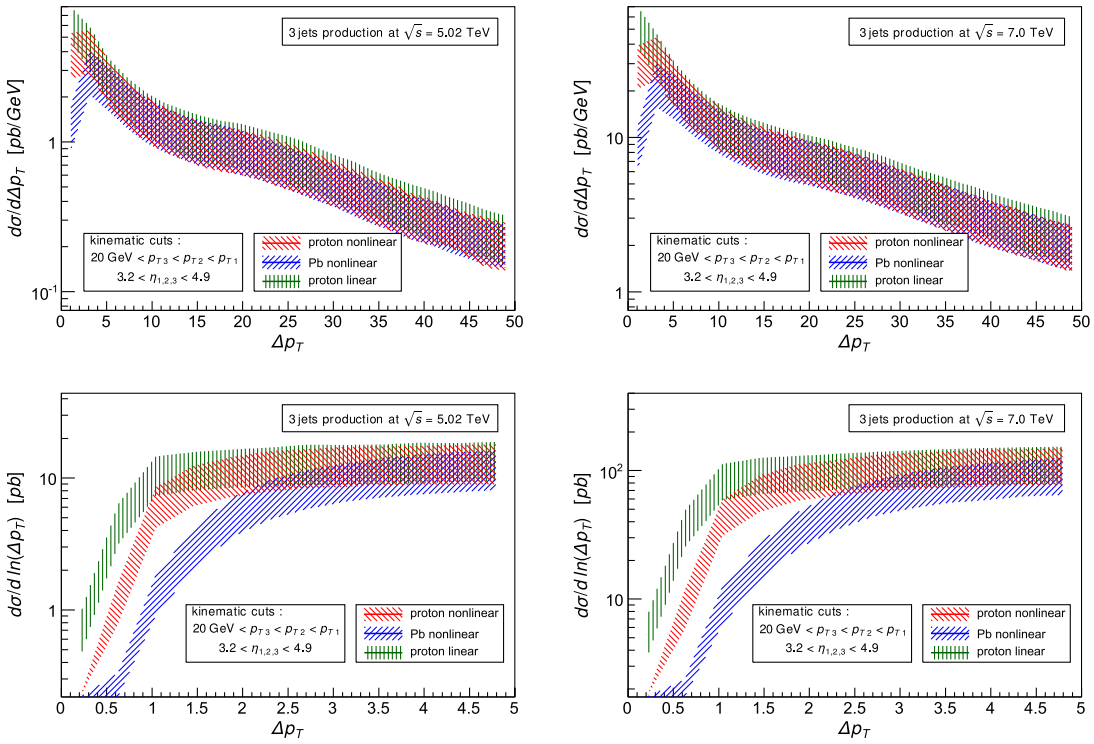

FIG. 17 (color online). Differential cross section in the unbalanced p_T for forward jets. The band represents the theoretical uncertainty due to scale variation and statistical errors. The left plots correspond to c.m. energy 5.02 TeV, the right to 7.0 TeV. The bottom plots zoom the low Δp_T region [note the distributions are in $\ln(\Delta p_T)$ there].

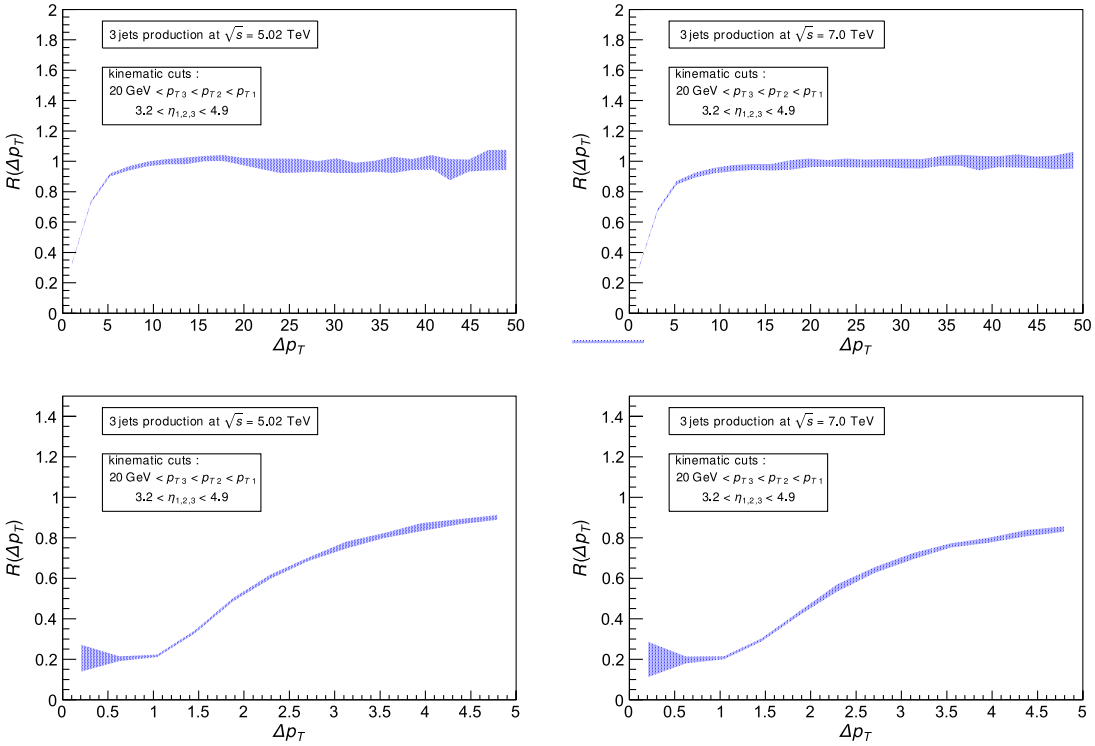

FIG. 18 (color online). The nuclear modification factor for forward jets as a function of the unbalanced p_T for regions close to zero. The band represents the theoretical uncertainty due to scale variation and statistical errors. The left plot corresponds to c.m. energy 5.02 TeV, right to 7.0 TeV. The bottom plots zoom the region close to zero.

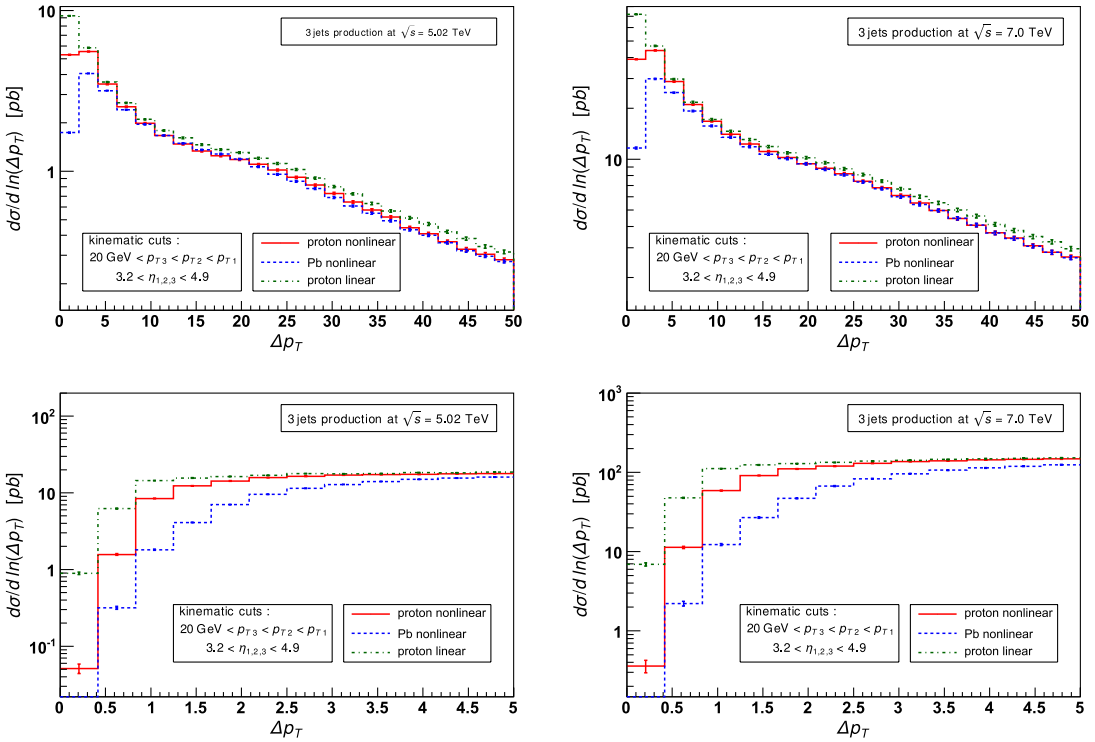

FIG. 19 (color online). Differential cross section for forward jets in the unbalanced p_T for a particular choice of the scale $\mu/2$. The left column corresponds to c.m. energy 5.02 TeV, the right to 7.0 TeV. The bottom plots zoom the top plots for the low Δp_T region [note the distributions are in $\ln(\Delta p_T)$ there].

calculation we choose $D_{\rm cut} = 30$ GeV. We have checked empirically that in order to observe any significant difference comparing to the forward-central case discussed above we should use $D_{\rm cut} < p_{T\rm cut}$. Our result are presented in Figs. 8–10. The main properties of the distributions are the following. First, the relative magnitude between the collinear region and the "noncollinear" region is decreased comparing to the previous case. This indicates that we enter the region which is small x sensitive. We see (right of Figs. 8 and 10) that for the c.m. energy of 7 TeV and the large energy scale, the distributions are different for linear and nonlinear evolution and the difference is most significant in the noncollinear region. The nuclear modification factor (Fig. 9) is, however, still consistent with unity.

2. Forward jets

Let us move to the case where all of the jets are in the forward rapidity region. As discussed in Sec. IV B, in this region we can safely go to relatively low values of $p_{T\rm cut}$; thus we set $p_{T\rm cut} = 20$ GeV. We present the results in Figs. 11–13. We observe significant differences between the three scenarios (nonlinear proton, nonlinear Pb, and linear proton) in the middle region of ϕ_{13} distributions, i.e., in the collinear region. It is also nicely illustrated by the nuclear modification ratios (Fig. 12) which now have two dips in that region, indicating that the region is sensitive to the nonlinear effects. The qualitative behavior is the same for both considered c.m. energies.

D. Unbalanced jet transverse momentum

Let us now switch to an analysis of the cross section as a function of the following quantity:

$$\Delta p_T = |\vec{p}_{T1} + \vec{p}_{T2} + \vec{p}_{T3}|, \tag{20}$$

which in the prescription given by the Eq. (4) corresponds to the transverse momentum of the off-shell gluon, i.e., $\Delta p_T = |\vec{k}_{TA}|$.

Let us remark that the distributions we are going to present can be much more affected by the final state parton shower, than the decorrelation distribution presented above. Nevertheless, it is very interesting to study the influence of different evolution equations for the multiparticle production purely within the high-energy factorization.

1. Central-forward jets

We present the results in Figs. 14–16. The first immediate observation is that the distributions possess a maximum around 1 GeV (bottom of Figs. 14 and 16) which corresponds to the maximum of the unintegrated gluon densities (see Ref. [20]) used in the calculations. The region below 1 GeV is sensitive to the different evolutions; the most significant difference is between linear and nonlinear evolution. However, the nuclear modification factor is slightly suppressed for $\Delta p_T < 2.5$ GeV.

The scenario with the two leading jets being back-to-back-like is not especially interesting for the unbalanced transverse momentum distributions due to the kinematics involved. It turns out that the region of Δp_T that is smaller then a few GeV is kinematically forbidden. Although back-to-back forward-central jets actually probe the high transverse momenta in the unintegrated gluon density, we did not see any conclusive features of tails in our distributions.

2. Forward jets

Finally we turn to the forward rapidity region. Again we note the significant differences in the distributions for different evolution scenarios (Figs. 17–19). They are most prominent in the low unbalanced transverse momentum region $\Delta p_T < 5$ GeV (see the bottom plots in Figs. 17–19). We note the suppression of the distributions with nonlinear evolution, with, however, lead being suppressed much more. This is also reflected in the nuclear modification ratios as is evident from Fig. 18. Interestingly, the nuclear modification factor is not so much sensitive to the scale variation.

V. SUMMARY

In the present work we have studied three-jet production at LHC for proton-proton and proton-lead collisions. As we pointed out, the trijet final state is an ideal tool to perform scans of small x unintegrated gluon density and to discriminate between different evolution scenarios. In our work we have used two independent Monte Carlo programs which implement high-energy k_T factorization with a single off-shell gluon and gauge invariant matrix elements. We have studied three scenarios for the evolution of the unintegrated gluon density: nonlinear evolution for proton and lead according to Refs. [59,60] and its linear version. From numerous observables that can be constructed for a three-jet process, we have chosen azimuthal decorrelations and the unbalanced transverse momentum of the jets. We considered two rapidity regions accessible experimentally: the forward-central region and the purely forward region. In addition we have considered the situation when the two central jets are back-to-back-like. Our findings can be briefly summarized as follows. Forward-central collisions with a relatively high cut on the transverse jet momenta are not sensitive to different kinds of gluon evolution, although they reflect some key features of the high-energy kinematics. The situation changes, when the two leading jets are approximately back to back as the distributions start to be sensitive to the region of a relatively large transverse momentum in the unintegrated gluon density. For the case of forward scattering, we observe a significant difference between all three kinds of evolution, in particular the shape of the nuclear modification factors (Figs. 12 and 18) suggest strong suppression due to saturation effects, which is visible both in the azimuthal decorrelations and the unbalanced p_T distributions.

ACKNOWLEDGMENTS

The authors are grateful to N. Armesto, P. Cipriano, S. Jadach, P. van Mechelen, W. Słominski, M. Strikman, and M. Trzebiński for discussions. This work was supported by the NCBiR Grant No. LIDER/02/35/L-2/10/NCBiR/2011.

[1] J. Collins, *Foundations of Perturbative QCD* (Cambridge University Press, Cambridge, England, 2011), Vol. 32.
[2] E. Kuraev, L. Lipatov, and V. S. Fadin, Sov. Phys. JETP **45**, 199 (1977).
[3] I. Balitsky and L. Lipatov, Sov. J. Nucl. Phys. **28**, 822 (1978).
[4] M. Ciafaloni, Nucl. Phys. **B296**, 49 (1988).
[5] S. Catani, F. Fiorani, and G. Marchesini, Nucl. Phys. **B336**, 18 (1990).
[6] S. Catani, F. Fiorani, and G. Marchesini, Phys. Lett. B **234**, 339 (1990).
[7] I. Balitsky, Nucl. Phys. **B463**, 99 (1996).
[8] Y. V. Kovchegov, Phys. Rev. D **60**, 034008 (1999).
[9] K. Kutak, K. Golec-Biernat, S. Jadach, and M. Skrzypek, J. High Energy Phys. 02 (2012) 117.
[10] K. Kutak, J. High Energy Phys. 12 (2012) 033.
[11] A. H. Mueller and H. Navelet, Nucl. Phys. **B282**, 727 (1987).
[12] V. Del Duca, M. E. Peskin, and W.-K. Tang, Phys. Lett. B **306**, 151 (1993).
[13] W. J. Stirling, Nucl. Phys. **B423**, 56 (1994).
[14] C. Marquet and C. Royon, Nucl. Phys. **B739**, 131 (2006).
[15] L. Gribov, E. Levin, and M. Ryskin, Phys. Rep. **100**, 1 (1983).
[16] A. H. Mueller and J.-w. Qiu, Nucl. Phys. **B268**, 427 (1986).
[17] A. Stasto, K. J. Golec-Biernat, and J. Kwiecinski, Phys. Rev. Lett. **86**, 596 (2001).
[18] J. L. Albacete and C. Marquet, Phys. Rev. Lett. **105**, 162301 (2010).
[19] A. Dumitru, K. Dusling, F. Gelis, J. Jalilian-Marian, T. Lappi, and R. Venugopalan, Phys. Lett. B **697**, 21 (2011).
[20] K. Kutak and S. Sapeta, Phys. Rev. D **86**, 094043 (2012).
[21] M. Deak, F. Hautmann, H. Jung, and K. Kutak, J. High Energy Phys. 09 (2009) 121.
[22] M. Deak, F. Hautmann, H. Jung, and K. Kutak, Eur. Phys. J. C **72**, 1982 (2012).
[23] D. Y. Ivanov and A. Papa, J. High Energy Phys. 05 (2012) 086.
[24] G. Chachamis, M. Hentschinski, J. Madrigal Martinez, and A. S. Vera, arXiv:1211.2050.
[25] M. Hentschinski and C. Salas, arXiv:1301.1227.
[26] S. Chatrchyan *et al.* (CMS Collaboration), J. High Energy Phys. 11 (2011) 148.
[27] V. Khachatryan *et al.* (CMS Collaboration), Phys. Rev. Lett. **106**, 122003 (2011).
[28] S. Chatrchyan *et al.* (CMS Collaboration), J. High Energy Phys. 06 (2012) 036.
[29] J. Collins and J.-W. Qiu, Phys. Rev. D **75**, 114014 (2007).
[30] T. C. Rogers and P. J. Mulders, Phys. Rev. D **81**, 094006 (2010).
[31] P. Mulders and T. Rogers, arXiv:1102.4569.
[32] F. Gelis, E. Iancu, J. Jalilian-Marian, and R. Venugopalan, Annu. Rev. Nucl. Part. Sci. **60**, 463 (2010).
[33] B.-W. Xiao and F. Yuan, Phys. Rev. Lett. **105**, 062001 (2010).
[34] F. Dominguez, C. Marquet, B.-W. Xiao, and F. Yuan, Phys. Rev. D **83**, 105005 (2011).
[35] L. D. McLerran and R. Venugopalan, Phys. Rev. D **49**, 2233 (1994).
[36] L. D. McLerran and R. Venugopalan, Phys. Rev. D **49**, 3352 (1994).
[37] Y. V. Kovchegov and K. Tuchin, Phys. Rev. D **65**, 074026 (2002).
[38] D. Kharzeev, Y. V. Kovchegov, and K. Tuchin, Phys. Rev. D **68**, 094013 (2003).
[39] E. Avsar, Int. J. Mod. Phys. Conf. Ser. **04**, 74 (2011).
[40] E. Avsar, arXiv:1203.1916.
[41] F. Dominguez, C. Marquet, A. M. Stasto, and B.-W. Xiao, Phys. Rev. D **87**, 034007 (2013).
[42] E. Iancu and D. Triantafyllopoulos, arXiv:1307.1559.
[43] J. P. Blaizot, F. Gelis, and R. Venugopalan, Nucl. Phys. **A743**, 13 (2004).
[44] H. Fujii, F. Gelis, and R. Venugopalan, Nucl. Phys. **A780**, 146 (2006).
[45] J. Kwiecinski, A. D. Martin, and A. Stasto, Phys. Rev. D **56**, 3991 (1997).
[46] S. Catani, M. Ciafaloni, and F. Hautmann, Nucl. Phys. **B366**, 135 (1991).
[47] S. Catani, M. Ciafaloni, and F. Hautmann, Nucl. Phys. B, Proc. Suppl. **18**, 220 (1991).
[48] S. Catani, M. Ciafaloni, and F. Hautmann, Phys. Lett. B **242**, 97 (1990).
[49] S. Catani and F. Hautmann, Phys. Lett. B **315**, 157 (1993).
[50] S. Catani, M. Ciafaloni, and F. Hautmann, Phys. Lett. B **307**, 147 (1993).
[51] S. Catani and F. Hautmann, Nucl. Phys. **B427**, 475 (1994).
[52] L. Lipatov, Nucl. Phys. **B452**, 369 (1995).
[53] E. Antonov, L. Lipatov, E. Kuraev, and I. Cherednikov, Nucl. Phys. **B721**, 111 (2005).
[54] M. Nefedov, V. Saleev, and A. V. Shipilova, Phys. Rev. D **87**, 094030 (2013).
[55] V. Saleev and A. Shipilova, Phys. Rev. D **86**, 034032 (2012).
[56] B. Kniehl, V. Saleev, A. Shipilova, and E. Yatsenko, Phys. Rev. D **84**, 074017 (2011).
[57] A. van Hameren, P. Kotko, and K. Kutak, J. High Energy Phys. 01 (2013) 078.
[58] A. van Hameren, P. Kotko, and K. Kutak, J. High Energy Phys. 12 (2012) 029.

[59] K. Kutak and J. Kwiecinski, Eur. Phys. J. C **29**, 521 (2003).
[60] K. Kutak and A. Stasto, Eur. Phys. J. C **41**, 343 (2005).
[61] A. Dumitru, A. Hayashigaki, and J. Jalilian-Marian, Nucl. Phys. **A765**, 464 (2006).
[62] M. Cacciari, G. P. Salam, and G. Soyez, J. High Energy Phys. 04 (2008) 063.
[63] S. Jadach, Comput. Phys. Commun. **152**, 55 (2003).
[64] T. Sjostrand, S. Mrenna, and P. Z. Skands, Comput. Phys. Commun. **178**, 852 (2008).
[65] A. Stasto, B.-W. Xiao, and F. Yuan, Phys. Lett. B **716**, 430 (2012).
[66] H.-L. Lai, M. Guzzi, J. Huston, Z. Li, P. M. Nadolsky, J. Pumplin, and C.-P. Yuan, Phys. Rev. D **82**, 074024 (2010).